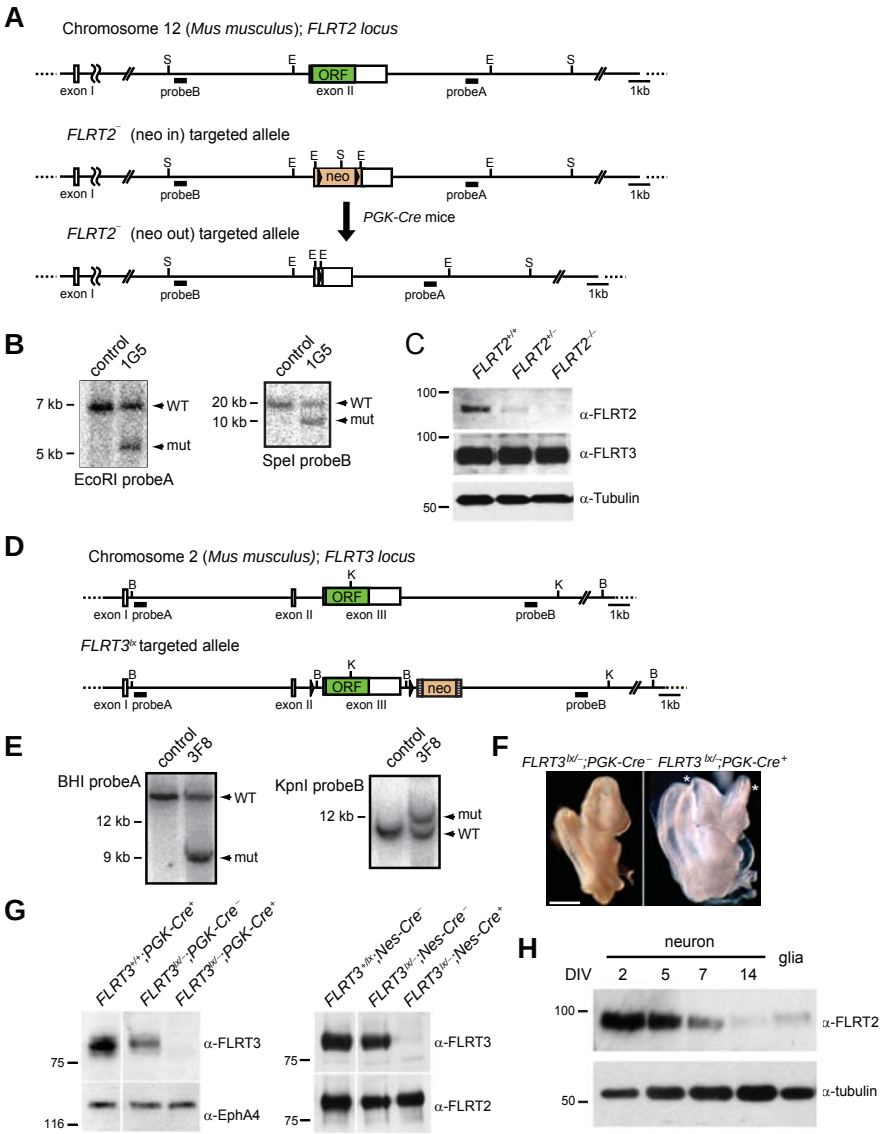

Supplementary Figure 1. Generation and validation of the FLRT2 knock-out and FLRT3lx conditional alleles. (**A**) Scheme of the FLRT2 knock-out allele generated by homologous recombination of exon II, containing the entire open reading frame (ORF), of the mouse FLRT2 gene. The FLRT2− allele exon II was replaced by a loxP-flanked PGK-driven neomycin gene. The neo cassette was later removed by crossing FLRT2+/− mice with the PGK-Cre line. (**B**) Southern blots showing homologous recombination on both 5' and 3' arms of the targeting vector in the ES cell clone 1G5 (FLRT2+/−) used for blastocyst injections. The relative position of the restriction sites EcoRI (E), SpeI (S), as well as that of the probes (probe A-B) used for genomic DNA digestion and hybridization are indicated in (**A**). (**C**) Western blot analysis showing FLRT2 protein levels in E17 brains of the indicated genotypes (anti-FLRT2-ECD antibody). Note the reduction of FLRT2 protein levels in heterozygotes and the absence of FLRT2 protein in FLRT2 −/−. FLRT3 and Tubulin were used as loading controls for the same samples. (**D**) Scheme of the FLRT3lx allele generated by homologous recombination in the mouse FLRT3 locus. Solid triangles flanking the exon III depict the loxP sites. (**E**) Southern blot showing homologous recombination on both 5' and 3' arms of the targeting vector in the ES cell clone 3F8 used for blastocyst injection. The relative position of the restriction sites BamHI (B) and KpnI (K) as well as that of the probes (probe A and B) used for genomic DNA digestion and hybridization are indicated in (**D**). (**F**, **G**) Validation of the functionality of the FLRT3lx allele in vivo. FLRT3lx/+ mice were crossed with the deleter Cre line PGK-Cre and embryos were collected at E9.5. (**F**, left) Frontal view of a control embryo with a closed neural tube. (**F**, right) Frontal view an embryo FLRT3lx/-;PGK-Cre+ showing the characteristic open head phenotype (asterisks) of the FLRT3-/- embryos (Egea et al., 2008). (**G**, left) Western blot analysis using lectin pull-down samples from embryos of the indicated genotypes. Note the complete absence of FLRT3 expression in FLRT3lx/-;PGK-Cre+ embryos. EphA4 was used as loading control. (**G**, right) FLRT3lx/+ mice were crossed with FLRT3+/− mice carrying the neuron specific Cre line, Nestin-Cre. Lectin pull-down samples of brain lysates of the indicated genotypes were analyzed by Western blot. FLRT3 was absent in FLRT3lx/-;Nestin-Cre+ brains. FLRT2 was used as loading control. (**H**) Low FLRT2 expression in glial cells. Western blot analysis of protein extracts from primary cultured neurons from E17 mouse hippocampus for the indicated DIV and glial cells. Extracts were analyzed with an anti-FLRT2-ECD antibody (upper panel) and with an anti-Tubulin antibody as loading control (lower panel).

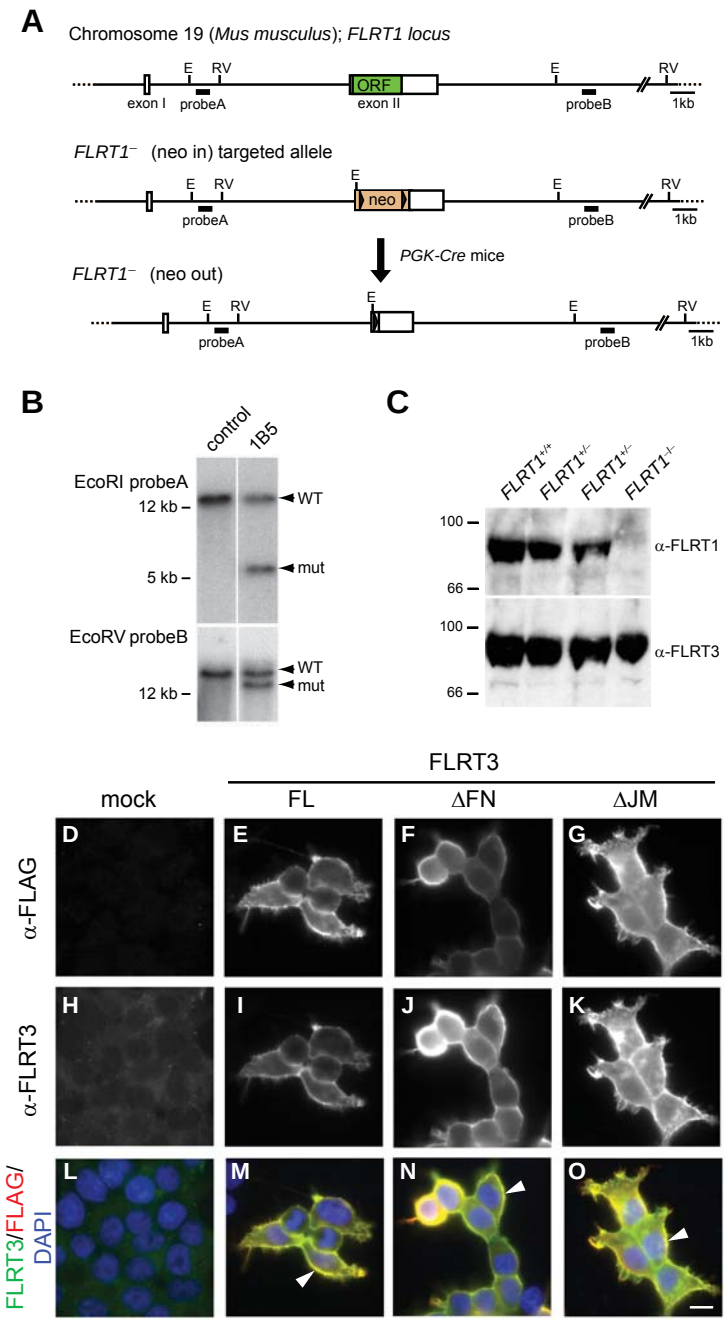

Supplementary Figure 2. Generation and validation of the FLRT1 knock-out allele and membrane localization of FLRT3 deletion mutants (**A**) Scheme of the FLRT1 knock-out allele generated by homologous recombination of exon II, containing the entire ORF of the mouse FLRT1 gene. Exon II was replaced by a loxP-flanked PGK-driven neomycin gene which was recombined in vivo by crossing with the deleter line PGK-Cre. (**B**) Southern blots showing homologous recombination on both 5' and 3' arms of the targeting vector in the ES cell clone 1B5 used for blastocyst injection. The relative position of the restriction sites EcoRI (E) and EcoRV (RV) as well as that of the probes (probe A and B) used for genomic DNA digestion and hybridization are indicated in (**A**). (**C**) Western blot analysis showing FLRT1 protein levels in lectin pull-down samples of brain lysates of the indicated genotypes. Note the reduction of FLRT1 protein levels in heterozygotes and the absence of FLRT1 protein in FLRT1-/-. FLRT3 was used as loading control in the same samples.

(**D-O**) HEK293T cells were transiently transfected with C-terminally FLAG tagged constructs of FLRT3 full length (FL), FLRT3 deletion mutant lacking the FNIII domain (ΔFN), FLRT3 deletion mutant lacking the juxtamembrane region (ΔJM) or control vector (MOCK). After one day, cells were fixed and stained with anti-FLAG (**D-G**) and anti-FLRT3 (**H-K**) antibodies (extracellular epitope for FLRT3). The merge of the two stainings is shown in **L-O** together with DAPI to visualize nuclei. Note the similar membrane distribution of the deletion constructs compared to FL (arrowheads in **M**, **N** and **O**). Scale bar, 10 µm

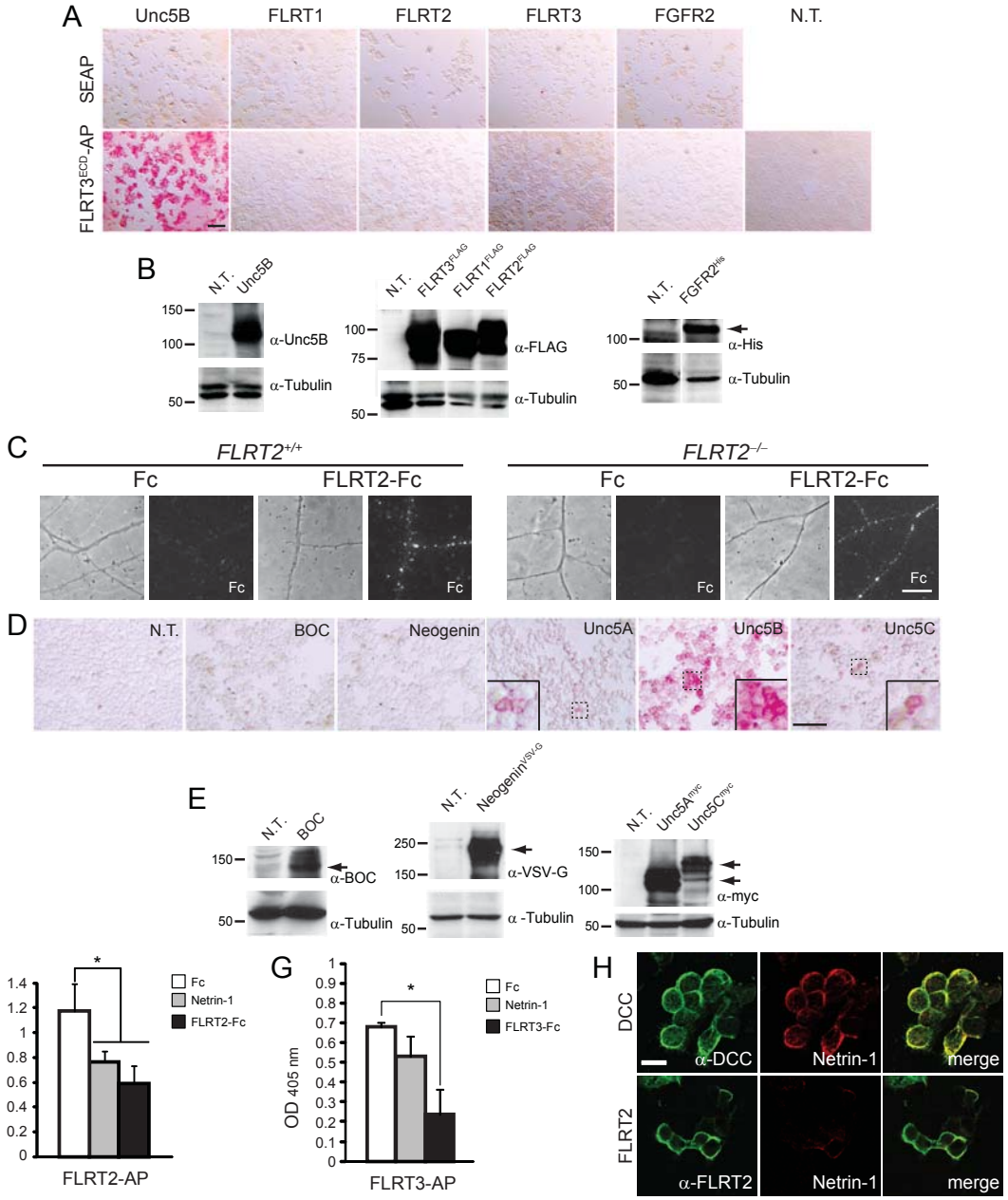

Supplementary Figure S3. Binding of the different FLRT/ECDs to candidate receptors. (**A,B**) FLRTs do not bind homo- or heterophilically. HEK293T cells were transiently transfected with Unc5B, FLAG-tagged FLRT1, FLRT2 and FLRT3, with His-tagged FGFR2 or left untransfected (N.T.). (**A**) After 2 DIV, cells were incubated with secreted alkaline phosphatase (SEAP) or FLRT3/ECD-AP, as indicated. Only cells overexpressing Unc5B show a significant binding to FLRT3/ECD. Scale bar in (**A**), 100 μm. (**B**) Correct expression of the transfected constructs was analyzed in protein lysates of sibling transfected cells by Western blot using specific antibodies. Tubulin was used as loading control. (**C)** Wild-type (+/+) or FLRT2−/− primary cultures of E17.5 hippocampal neurons (3DIV) were incubated for 30 minutes at 37°C with preclustered, recombinant Fc or FLRT2-Fc (1 μg/ml). Cultures were fixed and stained with anti-Fc to reveal FLRT2 binding sites. Fc alone did not give any staining above background. However, FLRT2-Fc incubation induced the formation of clusters in both wild-type and FLRT2−/− neurons. The corresponding bright field images are shown (left to the Fc staining). Scale bar in (**C**), 10 μm. (**D,E**) HEK293T cells were transiently transfected with BOC, Unc5B, VSV-G tagged Neogenin, myc-tagged Unc5A and Unc5C or left untransfected (N.T.), as indicated. Cells were incubated with FLRT3/ECD-AP as described above. Cells overexpressing Unc5A or Unc5C showed weak, but reproducible, binding to FLRT3/ECD. Insets show higher magnification images of boxed area. Scale bar in (**D**), 100 μm. (**E**) Correct expression of the transfected constructs was analyzed in protein lysates of sibling transfected cells by Western blot using specific antibodies. Tubulin was used as loading control. (**F,G**) Netrin-1 competes with FLRT2/ECD-AP for binding to Unc5D. HEK293T cells were transiently transfected with Unc5D (**F**) or Unc5B (**G**) and then incubated for 20 min at 37°C with Netrin-1 (90 nM), Fc (400 nM) or FLRT-Fc (80 nM) as indicated. Stimulation was stopped on ice and FLRT2-AP (54 nM, **F**) or FLRT3-AP (56 nM, **G**) added. After washing, cells were incubated with the AP substrate p-nitrophenylphosphate and activity measured after 90 min of reaction. The graphs show one representative experiment (n=2) and are the mean value of at least three independent wells per condition (*p<0.05, t-test). (**H**) Netrin-1 does not bind FLRT2. HEK293T cells were transiently transfected with DCC or FLRT2. Cells were then incubated with Alexa-594 labeled Netrin-1 (100nM) for 30 minutes at room temperature. After fixation cells were stained with anti-DCC or anti-FLRT2. Scale bar in (**H**), 20 μm.

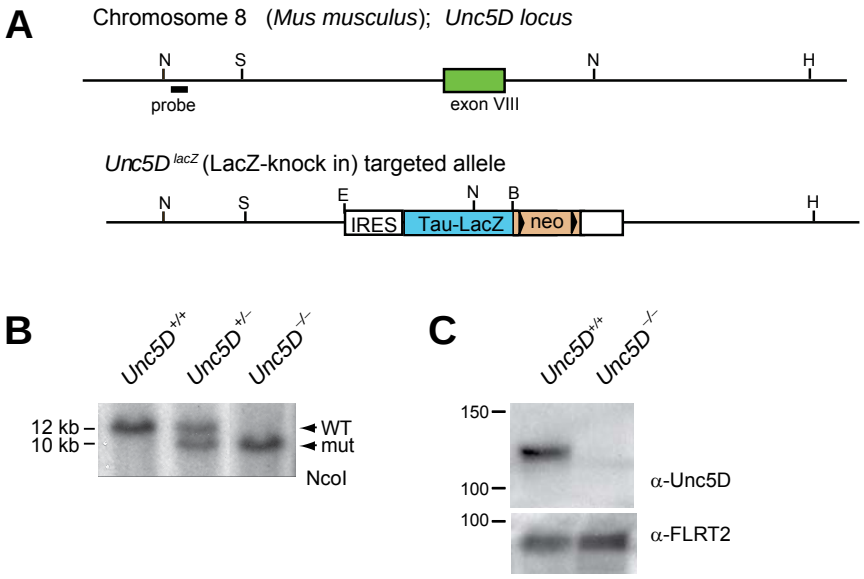

Supplementary Figure 4. Generation and validation of the Unc5D knock-out allele. (**A**) Scheme of the Unc5D knock-out alleles generated by homologous recombination of exon VIII of the mouse Unc5D gene. In the Unc5D− allele exon VIII was replaced by a IRES-Tau LacZ- neomycin gene, resulting in a missense mutation in the ectodomain of Unc5D protein. (**B**) Southern blots showing recombined allele in Unc5D+/- and Unc5D-/- lower band). The positions of restriction enzyme cutting sites for genomic DNA digestion by NcoI and the probe for hybridization are indicated in (**A**). (**C**) Western blot analysis using lectin pull-down samples showing Unc5D protein levels in adult brains of the indicated genotypes. Note the absence of Unc5D protein in Unc5D−/− tissue. FLRT2 was used as loading controls for the same samples.

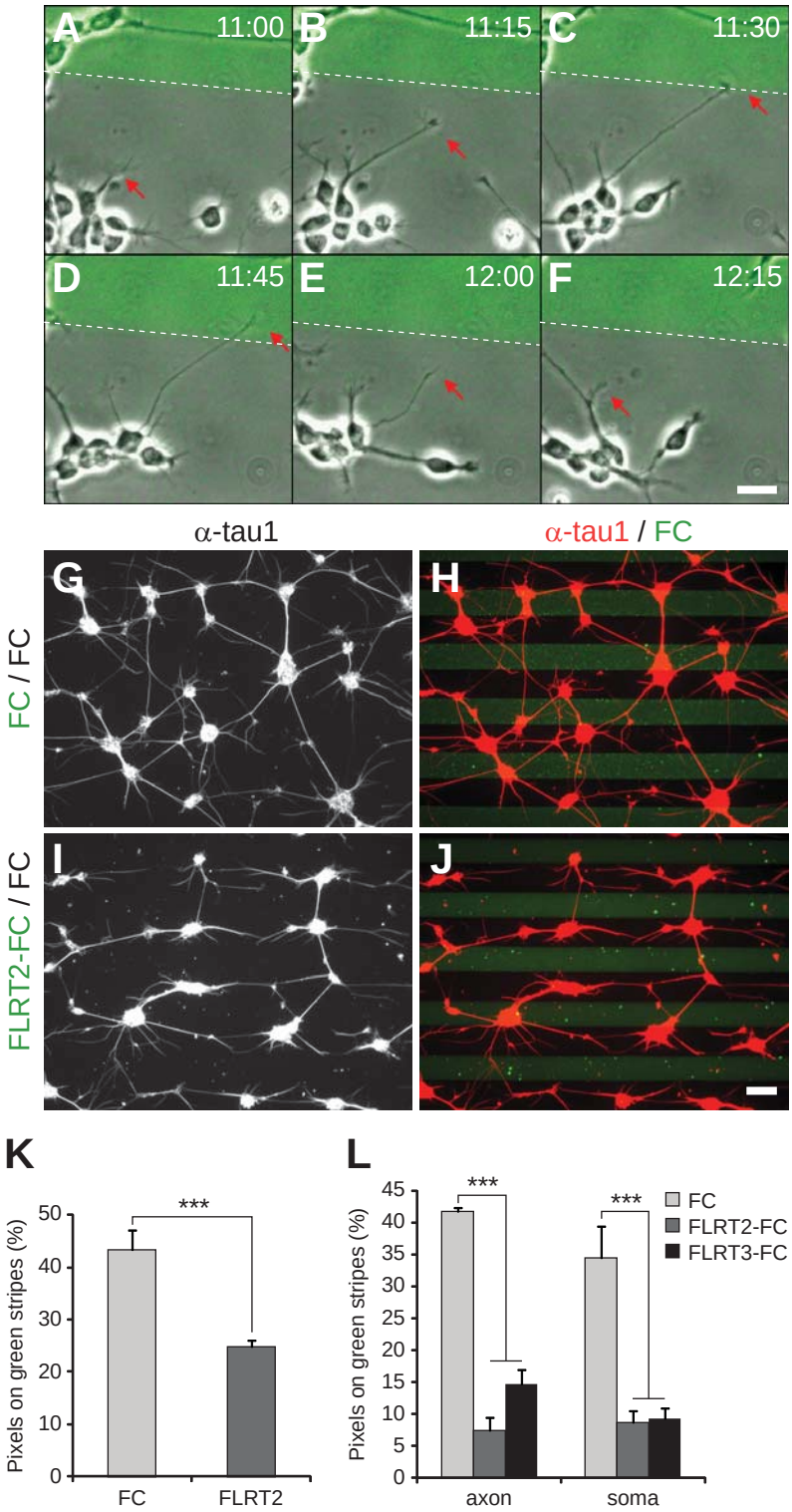

Supplementary Figure S5. FLRT2 and FLRT3 repel axons and soma of cultured neurons. (**A-F**) Axon repulsion induced by FLRT2-Fc on the stripe assay. Frames of a representative movie at different time points (h:m) showing the repulsive effect of FLRT2-Fc on one axon (red arrow) of dissociated hippocampal neurons (E15.5). The green stripe contains the FLRT2-Fc recombinant protein while the grey stripe contains the Fc control. The boundary between the two stripes is indicated by a stippled line. (**G-K**) FLRT2 has a repulsive effect on dissociated cortical neurons. E15.5 cortical neurons were grown on stripes containing control Fc (green) alternating with control Fc (black) (**G,H**) or FLRT2-Fc (green) alternating with control Fc (black) (**I,J**). Cells were stained with anti-tau1 antibody to visualize axons and cell bodies (red in **H,J**). Neurons on control stripes showed random outgrowth (**G,H**). FLRT2-Fc containing stripes had a repulsive effect on both axons and soma (**I,J**). Quantification of tau1+ pixels on green stripes showed a significant reduction of pixel localization on FLRT2-Fc stripes (25%) compared to control stripes (43%) (**K**). Results were obtained from two independent experiments (*** $p<0.001$, t-test). (**L**) Detailed analysis of axons and soma location in the stripe assay of Fig. 5G. Tau1+ pixels were separated into axons and cell soma. In control experiments (Fc), 42% of axonal pixels and 35% of somal pixels were on green stripes. In experiments with FLRT-Fc stripes, between 7 and 15% of pixels of both axons and soma were on green stripes (***$p<0.001$,t-test). Scale bars: (**A-F**) 20 μm, (**G-J**) 100 μm.

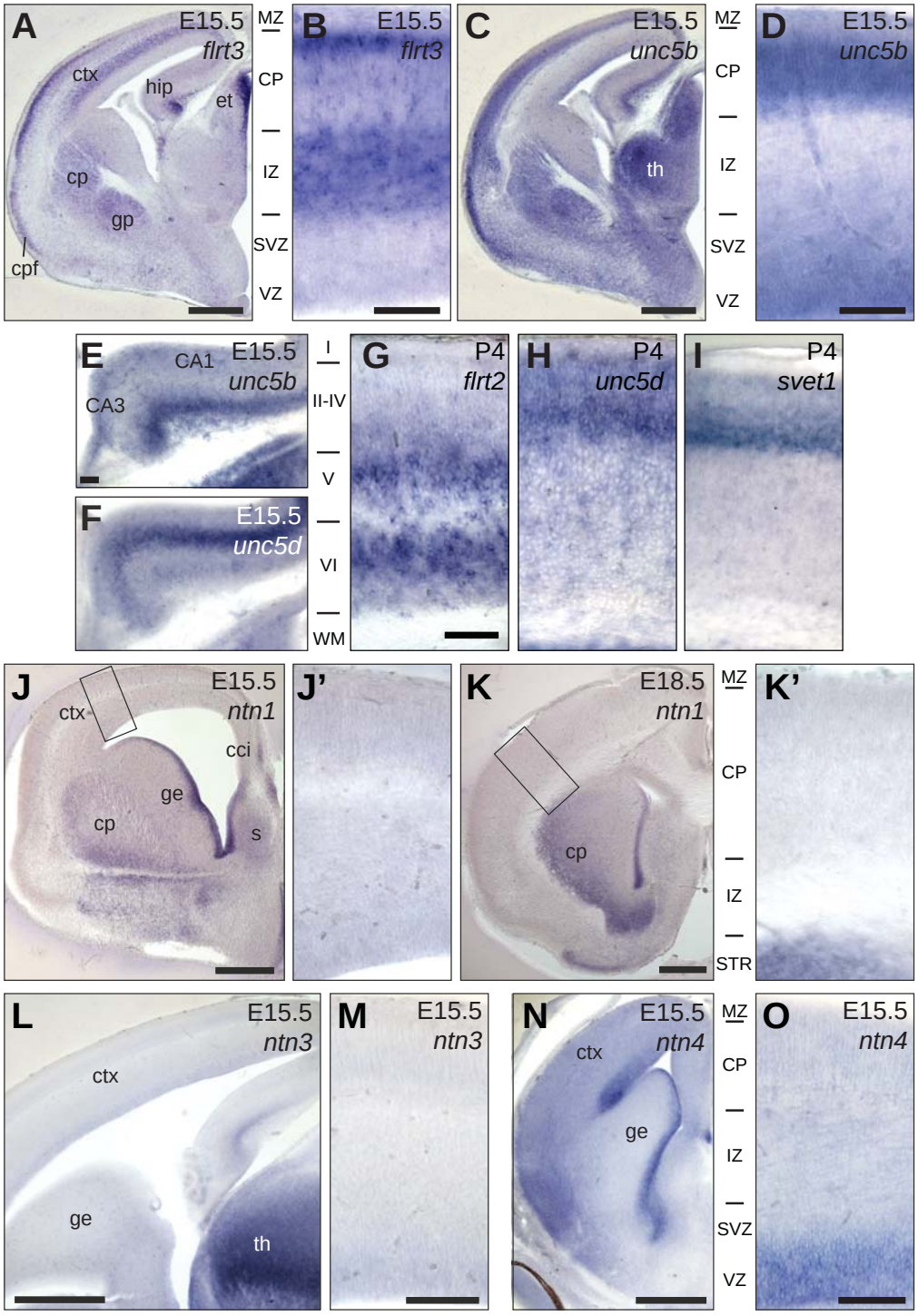

Supplementary Figure S6 Expression data of FLRT2, FLRT3, Unc5B, Unc5D, svet1, Netrin-1, Netrin-3 and Netrin-4 in the developing and early postnatal brain. In situ hybridization analyses of sagittal (**L,M**) and coronal (**A-K,N,O**) brain sections at the indicated developmental stages using the indicated digoxigenin-labeled antisense probes. Pictures show overviews of the brain (**A,C,J,K,L,N**), details of the hippocampus (**E,F**) or details of the dorsal neocortex (**B,D,G-I,M,O**). FLRT3 expression is detected in the piriform cortex, caudate putamen, globus pallidus, the CA3 region and dentate gyrus of the hippocampus and the ventricular zone of thalamus and epithalamus (**A**). In the cerebral cortex FLRT3 is expressed in the intermediate zone, in cells migrating through the cortical plate and in the upper layers of the cortical plate (**A,B**). Unc5B shows a strong expression in thalamus, globus pallidus, caudate putamen, piriform cortex, hippocampus and cerebral cortex (**C**) In the cortex, the ventricluar zone shows moderate and the cortical plate strong expression of Unc5B (**C,D**). (**E,F**) Unc5B and Unc5D are both expressed in the hippocampus. Unc5B shows stronger expression in CA3 (**E**). Unc5D is more abundant in CA1 (**F**). (**G-I**) FLRT2 and Unc5D/svet1 expression in the cortex does not overlap at early postnatal stages. FLRT2 expression is confined to layers V and VI (**G**), whereas Unc5D and svet1 expression is predominant in upper layers II-IV (**H,I**). Netrin-1 is not expressed in the dorsal cortex at E15.5 or E18.5 (**J',K'**), although it can be detected in the ventricular zone of the ganglionic eminence, caudate putamen, septum and cingulate cortex (**J,K**). Netrin-3 is strongly expressed in the thalamus and in moderate levels in the hippocampus (**L**). No Netrin-3 signal above background was detected in the cortex (**L,M**). Netrin-4 is expressed in the ventricular zones of the cortex and the ganglionic eminence (**N,O**) Abbreviations: cci, cingulate cortex; cp, caudate putamen; ctx, cortex; ge, ganglionic eminence; gp, globus pallidus; s, septum; th, thalamus; WM, white matter (and see legend of Figure 7). Scale bars: **B,D-I,M,O**, 100 μm; **A,C,J,K,L,N**, 500 μm.

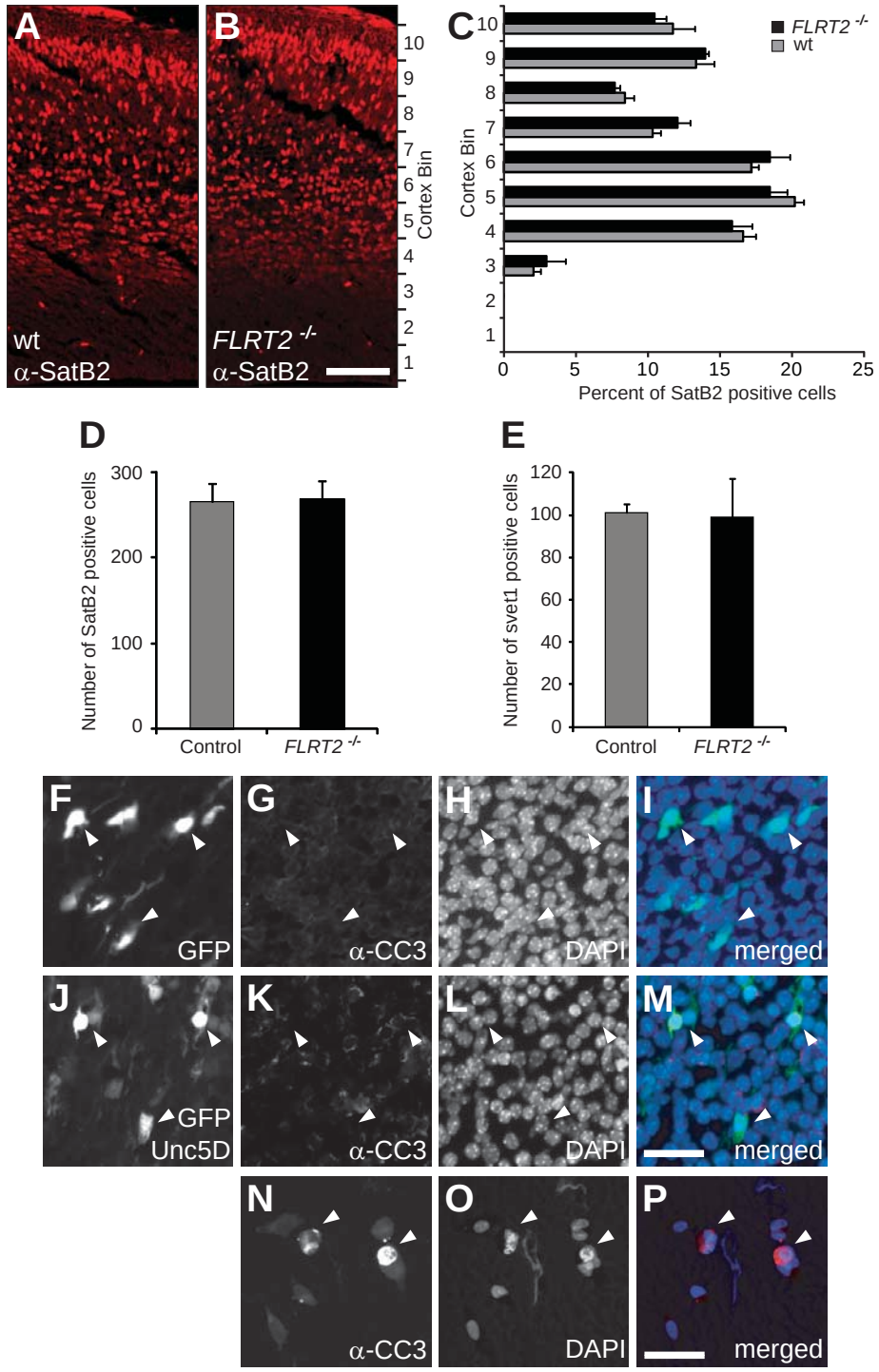

Supplementary Figure S7 Loss of FLRT2 accelerates radial migration of a subpopulation of cortical neurons in vivo, but does not affect cell survival. (**A-D**) SatB2 staining in coronal sections of rostral cortex at E15.5. (**A,B**) Representative images of wild-type and FLRT2-/- sections. (**C**) The region between VZ and pial surface was divided into 10 equally sized bins of 150 μm width and Satb2+ cells in each bin were counted. The average percentages of cells in each bin were calculated. No significant differences in cell distribution were found (Average +s.e.m., n=4 animals per group, t-test). (**D**) Compared to control mice, no significant difference in the total number of Satb2 positive cells in the lateral cortex were found in FLRT2-/- mice (Average +s.e.m., n=4 animals per group, t-test). (**E**) Loss of FLRT2 does not affect svet1 positive cell numbers in the lateral cortex (Average +s.e.m., n=3 animals per group, 3-7 sections per animal, t-test). (**F-P**) Unc5D overexpression in cortical neurons does not induce cell death. After in utero electroporation at E13.5 with GFP (**F-I**) or Unc5D-IREs-GFP (**J-M**) coronal sections of E17.5 cortex were stained with anti-active caspase 3 (CC3) to detect apoptotic cells. No double positive cells were detected in any of the conditions and tansfected cells did not show signs of nuclear fragmentation in the DAPI staining (arrowheads in **F-M** indicate location of transfected cells) (n=4 sections). (**N-P**) Quality control of the anti-active caspase 3 antibody. SH-SY5Y cells were treated with 1mM Paraquat to induce apoptosis. Apoptotic cells could be detected after fixation and staining with anti-active caspase 3 antibody (arrowheads **N-P**). Scale bars: (**A,B**) 100 μm, (**F-P**) 25 μm.

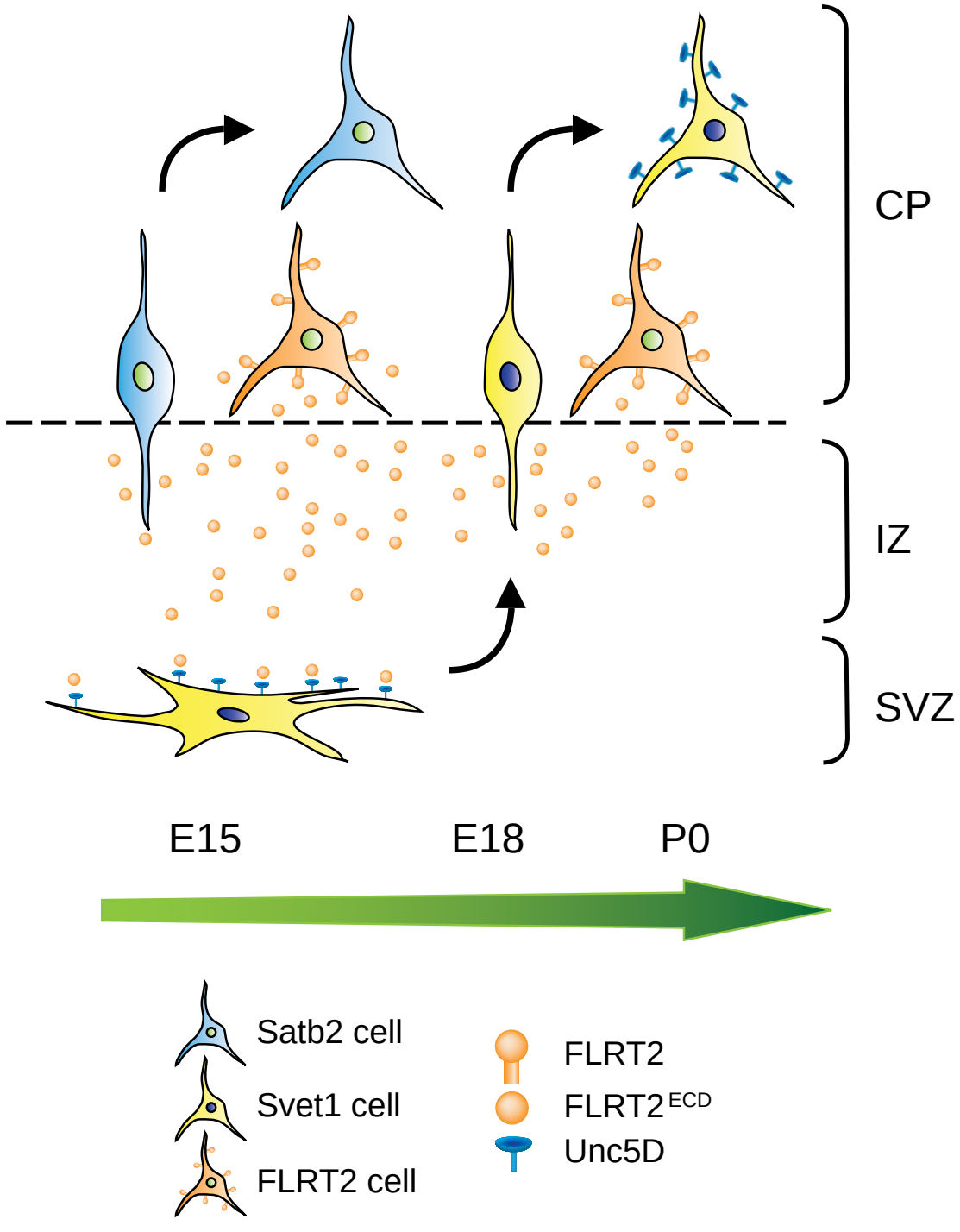

Supplementary Figure 8 Role of FLRT2 and Unc5D in radial migration. Satb2 cells migrate up toward to cortical plate (CP) immediately after neurogenesis. Conversely, the radial migration of multipolar Svet1+ (Unc5D+) cells in subventricular zone (SVZ) is inhibited by the ectodomain of FLRT2 which is shed by cells from the CP. Down regulation of Unc5D is observed in migrating Svet1+ cells which may be the mechanism that allows them to trespass the FLRT2 territory. After reaching upper cortical layers (mainly layer IV), Unc5D is re-expressed.

Supplementary Movie 1, related to Figure 5 and 6: Time lapse movie of dissociated neuron on stripe (FLRT2-Fc and control Fc).

Dissociated E15.5 hippocampal neurons were plated and grown on stripes containing FLRT2-Fc (green) versus control Fc. Images were taken every 15 min from 2 to 14 hr after plating. Neurons were dynamically moving and migrating away from FLRT2-Fc stripe. At the end of the movie, the cell shown in Figure 6**D** is repelled from FLRT2-Fc.

Supplementary Movie 2, related to Figure 5 and 6: Time lapse movie of dissociated neuron on stripe (control Fc and control Fc).

Neurons were prepared as described in Movie S1 and plated on stripes containing control Fc (green) versus control Fc. Images were taken as in Movie S1. Neurons dynamically movie and do not show a preferential distribution in any of the stripes.

Supplementary Materials and Methods

In utero electroporation

In utero electroporations at E13.5 were performed as previously described (Calegari et al, 2004). Anesthetized timed-pregnant mice were surgically operated to access the uterus. 1-3 μl DNA was injected into the ventricle with the pump controlled micropipette. After injection, six 50 ms electric pulses were generated with electrodes confronting the uterus above the lateral ventricles. The abdominal wall and skin were sewed and the mice were left until the appropriate embryonic stage.

In situ hybridization

For in situ hybridization, sections of brain tissue (80 μm thick) were collected with a Vibratome (Leica Microsystems). In situ hybridization was performed as previously described (Egea et al, 2008). For the FLRT2 riboprobe, mFLRT2 ecto- and transmembrane domain coding sequence was cloned into pcDNA3 vector. For the Unc5D riboprobe, a sequence containing 901 bp of coding and 3' UTR of mUnc5D (bp 2618-3519) was cloned into pCR-II-TOPO vector (Invitrogen). Same was done for the Unc5B riboprobe (818 bp of mUnc5B CDS and 3' UTR, bp 3016-3834). For the Netrin-1 riboprobe, a 400 bp sequence of mNetrin-1 (bp 1690-2089) was cloned into pGEM-T easy vector (Promega). For the Netrin-4 riboprobe, a 480 bp sequence of mNetrin-4 (bp 1805-2285) was cloned into pGEM-T easy vector (Promega). The svet1 (Tarabykin et al., 2001) and Netrin-3 ISH probes were described (Wang et al, 1999). Antisense- and sense-riboprobes were synthesized by SP6 and T7 RNA polymerase.

Immunostaining

For immunohistochemistry, embryos were collected from timed pregnant females and the brains were dissected, fixed in 4% PFA in PBS over night at 4°C and washed three times in PBS. For cryosections, brains were cryoprotected in 30% sucrose in PBS over night at 4°C and embedded in OCT. For anti-FLRT2 staining, brains were not cryoprotected. For paraffin sections, brains were dehydrated in an ascending ethanol series and 3 steps in Histo Clear (National Diagnostics). Brains were then immersed in paraffin for 36 hours with two changes of paraffin. Sections of 10 μm thickness were collected in a microtome. For immunofluorescence, sections were dewaxed and rehydrated, post-fixed in 4% PFA in PBS, washed in PBS and antigen retrieval was performed by boiling in 10 mM Sodium Citrate Buffer pH 6 with 0.05 % Tween two times for 3 min (Microwave, 900 W). After cooling down, sections were washed in PBS, permeabilized using 0.3% Triton X-100/PBS for 20 min and unspecific binding sites were blocked using 0.1% Triton X-100 5% donkey serum/PBS for 30 min. Sections were incubated with indicated

antibodies over night at 4°C in PBS with 0.1% Triton X-100 and 1% donkey serum. After washing with PBS, signal was detected with fluorescently labeled secondary antibodies. 20 µm cryosections (10 µm for in-utero electroporated brains) were permeabilized, blocked and incubated with indicated antibodies as described above. For enzymatic detection, sections were washed after the primary antibody step and incubated for 1 hr with biotinylated secondary antibodies that were visualized by the ABC method (Vector) with diaminobenzidine (DAB).

Primary culture of neurons and purification of the Fc fusion proteins

Mouse neurons were prepared from the hippocampus, cortex or motor cortex of E15.5-E16.5 embryos and maintained in Neurobasal plus B27 supplement (Invitrogen). Growth cone collapse was performed as previously described (Kullander et al, 2001). Preparation of rat cortical cultures (E16.5-18.5), nucleofection, RNAi knock down and growth cone collapse assays were performed according to previously published procedures (Hata et al, 2009). Fc fusion proteins were expressed in HEK293 cells and purified with protein A sepharose column using the AKTA system (Amersham); RGMa, Unc5B-ECD, Unc5D-ECD and FLRT2-His were purchased (R&D Systems).

Immunofluorescence in transfected HEK293T cells

Cells were transfected as above with the indicated constructs. After 24-36 h, cells were fixed and permeabilized. For Netrin-1 binding, Netrin1 (R&D Systems) was fluorescently labeled with the Alexa Fluor 594 Microscale Protein Labeling Kit (Molecular Probes) and incubated with the cells for 30 minutes at room temperature. Cells were then fixed but not permeabilized. Cells were then incubated with either anti-FLRT2 ECD or anti-FLRT3 ECD (R&D Systems), anti-DCC (1/1000, R&D Systems), anti-FLAG (Biomeda) or anti-hFc (Jackson ImmunoResearch) and the appropriate secondary antibodies (Jackson ImmunoResearch). DAPI was included after secondary antibody incubation in order to visualize nuclei. For the relative binding of Unc5B/D-Fcs to FLRT2/3-transfected cells the Fc signal (bound protein) was normalized to the total amount of expressed receptor (anti-FLAG staining) and expressed as arbitrary units.

Bibliography

Calegari F, Marzesco AM, Kittler R, Buchholz F, Huttner WB (2004) Tissue-specific RNA interference in post-implantation mouse embryos using directional electroporation and whole embryo culture. *Differentiation; research in biological diversity* **72:** 92-102

Egea J, Erlacher C, Montanez E, Burtscher I, Yamagishi S, Hess M, Hampel F, Sanchez R, Rodriguez-Manzaneque MT, Bosl MR, Fassler R, Lickert H, Klein R (2008) Genetic ablation of FLRT3 reveals a novel morphogenetic function for the anterior visceral endoderm in suppressing mesoderm differentiation. *Genes & development* **22:** 3349-3362

Hata K, Kaibuchi K, Inagaki S, Yamashita T (2009) Unc5B associates with LARG to mediate the action of repulsive guidance molecule. *The Journal of cell biology* **184:** 737-750

Kullander K, Mather NK, Diella F, Dottori M, Boyd AW, Klein R (2001) Kinase-dependent and kinase-independent functions of EphA4 receptors in major axon tract formation in vivo. *Neuron* **29:** 73-84

Wang H, Copeland NG, Gilbert DJ, Jenkins NA, Tessier-Lavigne M (1999) Netrin-3, a mouse homolog of human NTN2L, is highly expressed in sensory ganglia and shows differential binding to netrin receptors. *The Journal of neuroscience : the official journal of the Society for Neuroscience* **19:** 4938-4947